Available online at www.sciencedirect.com

ScienceDirect

Journal of Magnesium and Alloys 1 (2013) 341−345
www.elsevier.com/journals/journal-of-magnesium-and-alloys/2213-9567

Original research article

Bulk and local textures of pure magnesium processed by rotary swaging

W.M. Gan [a,*], Y.D. Huang [a], R. Wang [b], Z.Y. Zhong [b], N. Hort [a], K.U. Kainer [a], N. Schell [a], H.-G. Brokmeier [a,b], A. Schreyer [a]

[a] *Institute of Materials Research, Helmholtz-Zentrum Geesthacht, Max-Planck-Str. 1, D-21502 Geesthacht, Germany*
[b] *Institute for Materials Science and Engineering, Clausthal University of Technology, Agricolastrasse 6, D-38678 Clausthal-Zellerfeld, Germany*

Received 15 November 2013; accepted 25 December 2013

Abstract

Rotary swaging processing on commercial as-cast pure Mg has been carried out. Bulk texture variation with the processing passes was investigated using large gauge volume by neutron diffraction, of which results showed a combination of different components such as {00.2} basal fibre and two weak {10.0} and {11.0} fibres. Asymmetric distribution of the basal fibre around swaging direction was observed and being related to the processing parameters. Texture gradient analysis by synchrotron radiation demonstrates a non-uniform deformation of the RS processed pure Mg from surface to the centre.
Copyright 2014, National Engineering Research Center for Magnesium Alloys of China, Chongqing University. Production and hosting by Elsevier B.V. Open access under CC BY-NC-ND license.

Keywords: Rotary swaging; Pure magnesium; Bulk and local textures

1. Introduction

Rotary swaging (RS), a hammer forging process for the reduction of cross section of rods, tubes and wires, can lead to substantial grain refinement and corresponding enhancement of the mechanical properties for metals and alloys [1,2]. The low tooling cost and fast setup make swaging economical for production easy up to hundreds of pieces. Swaging products of Al alloy, steel and Cu alloy have been widely used but not many of Mg or magnesium alloys till nowadays [3,4].

Efforts have being taken to improve the mechanical properties of Mg and its alloys since they have high potential applications [5]. Conventional rolling and extrusion on Mg can help to improve the tensile properties, but the deformed Mg always exhibits a high strong anisotropy [6,7]. Researches of severe plastic deformation, such as equal channel angular pressing (ECAP) and high pressure torsion (HPT) on Mg and its alloys have been widely performed [8,9]. Swaging deformation on Mg and its alloys has not been so far widely carried out nevertheless it is a traditional forming technology.

Together with the microstructure polycrystalline materials are characterized by their texture − the distribution function of the crystallographic orientations of grains in relation to the sample coordinate system. Texture analysis is essential to study anisotropic behaviour and to optimise technological processes in applied as well as in fundamental researches. Texture analysis with conventional X-ray and EBSD has the disadvantages of difficult sample preparation and not enough grains statistics for ODF calculation. With neutron diffraction bulk samples rather than surfaces are measured, coarse-grained materials can be characterized easily [10]. Hard X-ray or synchrotron radiation shows relatively high resolution which offers a fast local/gradient texture investigation.

* Corresponding author.
E-mail addresses: weimin.gan@hzg.de, weimin.gan@gmail.com (W.M. Gan).
Peer review under responsibility of National Engineering Research Center for Magnesium Alloys of China, Chongqing University

Production and hosting by Elsevier

2213-9567 Copyright 2014, National Engineering Research Center for Magnesium Alloys of China, Chongqing University. Production and hosting by Elsevier B.V. Open access under CC BY-NC-ND license.
http://dx.doi.org/10.1016/j.jma.2013.12.004.

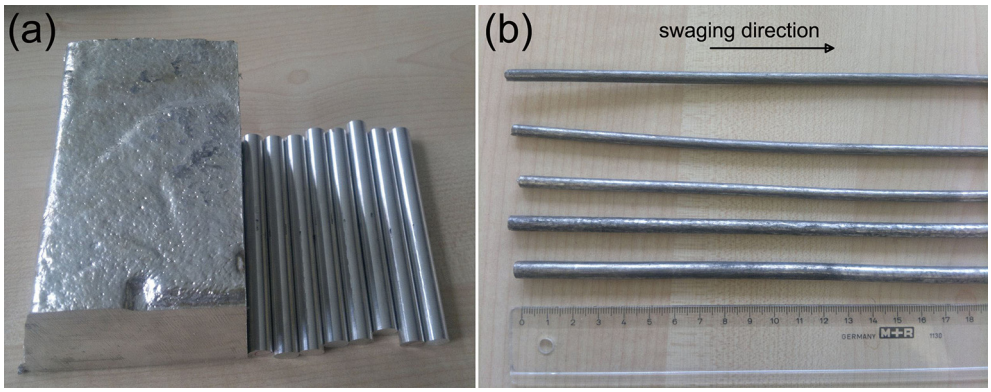

Fig. 1. (a) The start rods and (b) the specimens after RS processing.

Table 1
List of the sample information.

Sample	Processed temperature, °C	Diameter, mm	Deformation degree
S1	300	10.02	0.00
S2	300	8.60	0.31
S3	280	6.80	0.78
S4	280	6.05	1.01
S5	250	4.90	1.43
S6	250	4.55	1.58
S7	Room temperature	4.55	1.58

Current study is aimed to investigate the texture evolution under RS processing. Bulk and local textures will be related to the RS processing deformation mechanism.

2. Experimental

Commercial pure magnesium (99.99%) ingot was used as raw material, from which rods with dimension of Ø 10 mm × 100 mm height were machined as the start samples for swaging, as shown in Fig. 1(a). A stationary spindle swaging machine from Heinrich Müller was used. The sample was heated to the desired temperature and held for 10 min before each swaging. The heating temperature selected was gradually decreased, as listed in Table 1. A set of molds was used which produce gradual decrease for the final work piece from Ø 10 mm to Ø 4.5 mm, as shown in Fig. 1(b) a macro view of the swaged samples. The various deformation degree and, the true strain calculated from area reduction $\varphi = \ln (A_0/A)$, is listed in Table 1

Bulk texture evolution of the swaged samples was measured using the thermal neutron diffractometer STRESS-SPEC located at the FRM II, Heinz Maier–Leibniz Zentrum (MLZ) Garching, Germany [11]. These samples were directly machined from the swaged rod with a height of 10 mm. Five complete pole figures were measured using two detector positions with a wavelength of 1.70 Å. The new robot system was utilized to hand and to rotate the specimens, as shown in Fig. 2(a).

Texture gradient from the surface to the centre of the rod was analysed using synchrotron radiation at High Energy Materials Science Beamline P07 at PETRA III, DESY Germany. The beam size was 500 μm × 500 μm, a shown in Fig. 2(b) the macro view of the experimental setup. The measured position will be shown detailed in the following section. The measured pole figures from both instruments were calculated using the SteCa software [12].

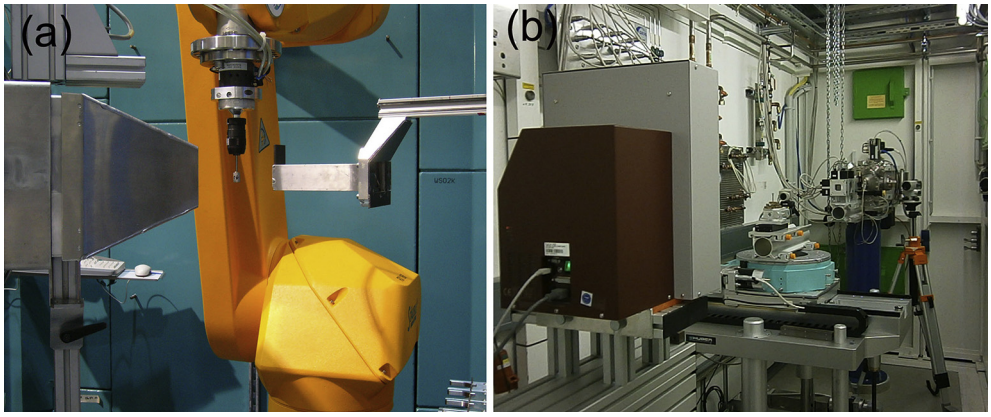

Fig. 2. (a) Setup of the neutron measurement at STRESS-SPEC; (b) setup of the synchrotron measurement at side station of HEMS.

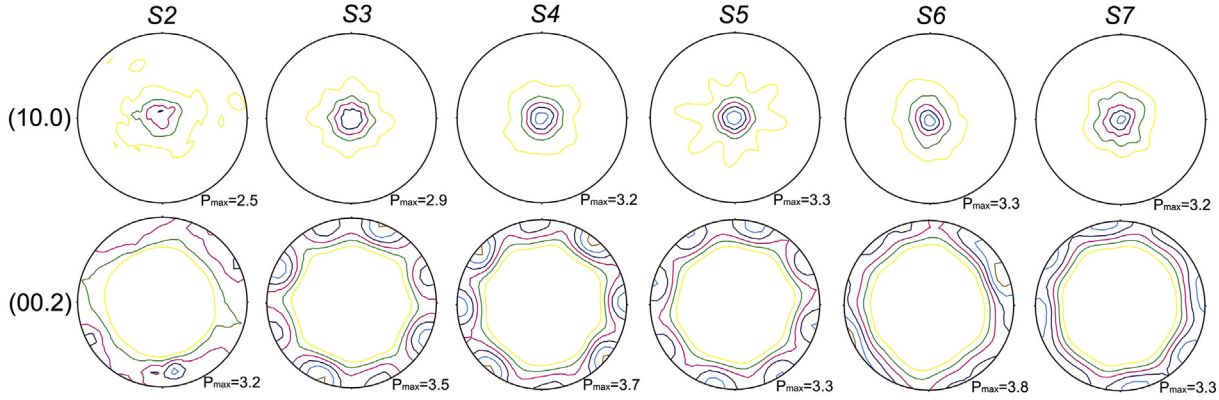

Fig. 3. Evolution of the (10.0) and (00.2) pole figures (counter levels = 1.0×, 1.5×, …) (swaging direction is at the pole figure center).

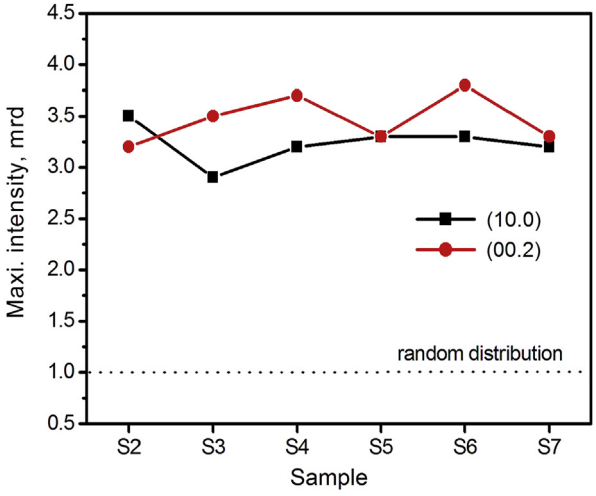

Fig. 4. Plot of the maximum intensity in the pole figures.

3. Results and discussions

The complete (10.0) and (00.2) pole figures of the samples S2 to S7 are shown in Fig. 3, respectively. The swaging direction is in the pole figure center. There exists a main {00.1} basal fiber at the first stage for the sample S2, which is similar to a typical hot compression or forging texture. In between two weak fibres {10.0} and {11.0} of the prismatic planes are also observed. These two components should come from the reheat treatment. These prismatic planes slip should also be accommodated by the compression twinning because the basal planes are already re-orientated for the input of S2. As for the sample S3 which was 4 times swaged from the sample S2 the maximum intensity is increased. From S4 (Ø 4.90 mm) to S5 and then to S6 (Ø 4.55 mm) with 250 °C preheating before swaging, S6 exhibits a little higher maximum basal intensity than that of S5. As for S7 which has the same diameter as the sample S6 but swaged at room temperature; its maximum intensity decrease with the recrystallization component more obvious compare to S6.

Fig. 4 plots the maximum intensity in these two pole figures of each sample. This apparently shows a slightly texture variation. It should be mentioned here that the (00.2) pole figure of S2 to S5 does not show a perfect round symmetry. This should come from the inhomogeneous feeding speed of the rod during swaging. Ideal case is that the most basal planes should be parallel to the forging direction with a homogeneous distribution [13]. There could lead to a texture gradient from surface to the rod center, which will be investigated thereafter.

Optical microstructure observations on the swaging processed samples indicated an inhomogeneous distribution from

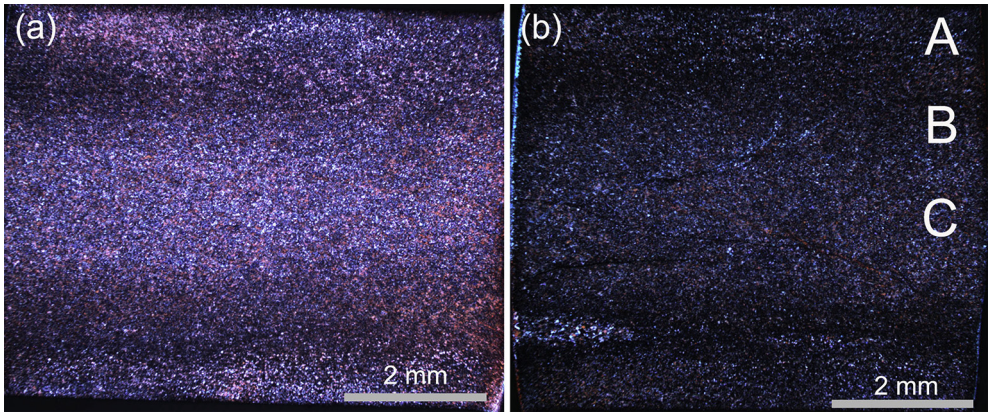

Fig. 5. Optical microstructures of samples (a) S6 and (b) S7, respectively.

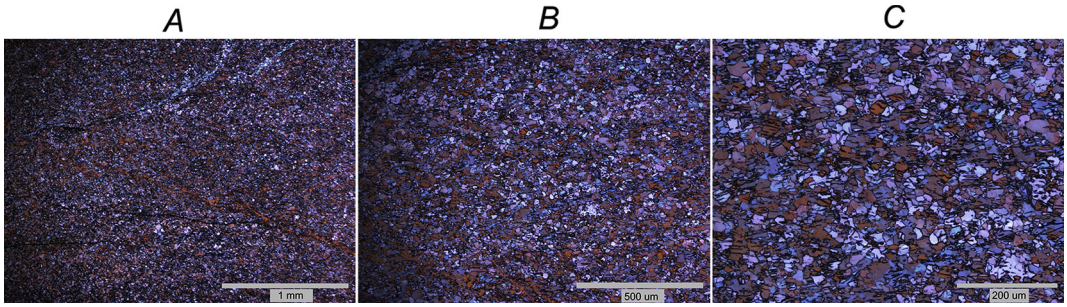

Fig. 6. Optical microstructure at the different positions marked in Fig. 5.

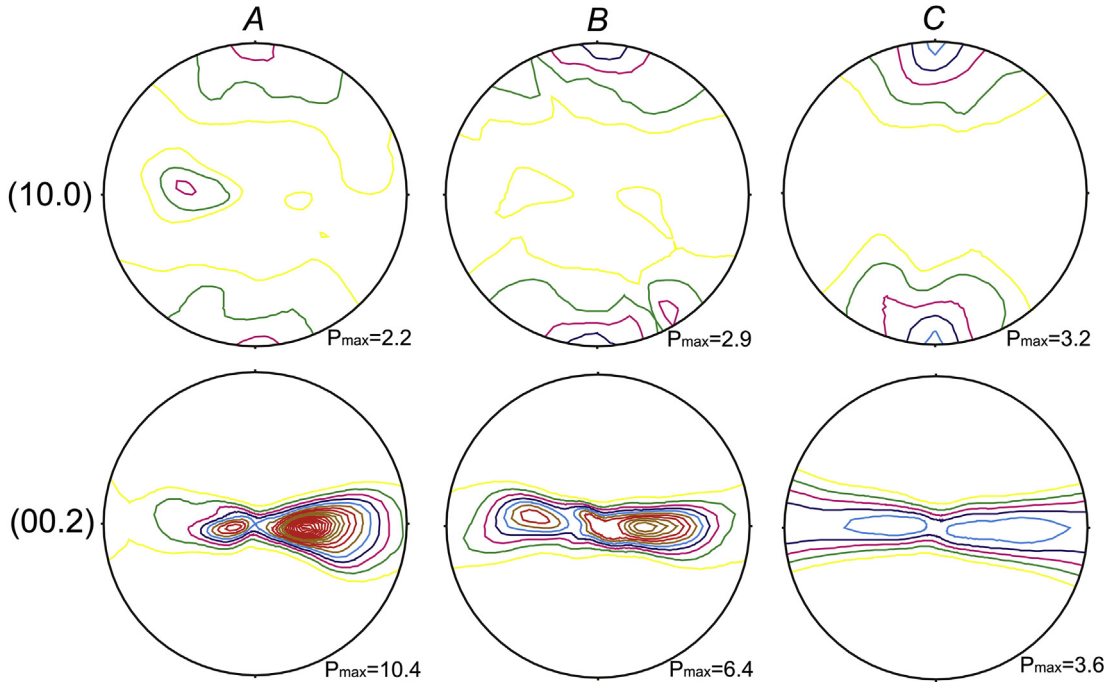

Fig. 7. (10.0) and (00.2) pole figures at positions A, B and C, respectively (counter levels = 1.0×, 1.5×, …) (swaging direction is to the top of pole figure).

surface to the centre in the rod. Typical OMs are found in Sample S6 (Fig. 5(a)) and S7 (Fig. 5(b)). The magnified microstructures of the marked positions (A, B and C) in S7 are shown in Fig. 6, respectively. Near surface region A exhibited a shear band. While position C shows fully recrystallized grains.

Therefore texture gradient analysis was performed. The specimen for synchrotron radiation was Ø4.55 × 4.55 mm^2 (S7). The measured (10.0) and (00.2) complete pole figures of the three positions are shown in Fig. 7, respectively. Common is that all the three positions show a basal fibre type texture. However, at the positions A and B the basal planes in some grains are re-orientated about 45° to the axial direction. This is much more obvious at the position A. According to the microstructures shown in Fig. 6 both the positions A and B have shearing bands.

Inhomogeneous distributions of the texture represent the non-uniform deformation along the diameter from surface to center of the swaging processed rod. Fig. 8 shows the diffraction peak (10.1) and (10.2) with their vector parallel to

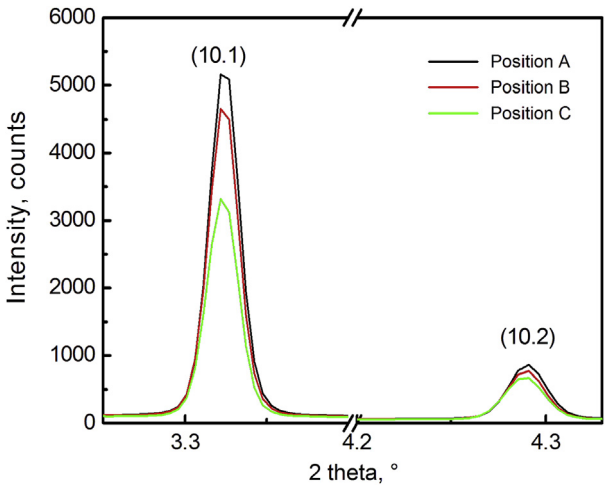

Fig. 8. Diffraction peaks of (10.1) and (10.2) from three different positions as marked in Fig. 5.

forging direction. Clear is that there exits peak shift from position A to B which should come from the high residual stress at near surface region.

Existence of the shear band near the surface should mainly result from the different rod feeding speed at each cycle and the friction between the die and rod. Since the rod was manually fed using the available swaging machine it is hard to keep a constant and uniform feeding speed. Moreover, the unavoidable gradient temperature distribution from surface to the rod center could also contribute to the microstructural inhomogeneity. However, this inhomogeneity is tending to decrease with the increase of swaging process cycle due to lowering the deformation temperature. This is one reason why we decrease the swaging temperature gradually. Moreover, continuously lowering the temperature could also contribute to the stability of microstructure, as reported by the ECAP processed Al−Mg alloy [14].

4. Summary

Advanced large neutron and synchrotron facilities take more advantages for bulk and local/gradient texture analysis, respectively, which plays an important role in deformed material. There exists a main {00.2} basal fiber texture in RS processed Mg. Basal planes are tended to be more homogeneous to be parallel to the RS direction with the increase of process pass. Texture is slightly inhomogeneous from the surface to the center of rods which indicates a non-uniform deformation, which could be due to the surface friction, temperature gradient, the die rotation speed, etc.

References

[1] F. Grosman, A. Piela, J. Mater. Process. Technol. 56 (1996) 404.
[2] T. Lyman, Forming, Metals Handbook, eighth ed., American Society for Metals, Ohio, 1969.
[3] M.A. Abdulstaar, E.A. El-Danaf, N.S. Waluyo, L. Wagner, Mater. Sci. Eng. A565 (2013) 351.
[4] P.N. Klau, L. Brandaob, F. Ortiz, O. Egungwu, F. Ige, Scrip. Mater. 38 (1998) 1755.
[5] N. Hort, Y.D. Huang, T.A. Leil, P. Maier, K.U. Kainer, Advan. Eng. Mater. 8 (2006) 359.
[6] H.-G. Brokmeier, W.M. Gan, M.Y. Zheng, Z. Zuberova, Y. Estrin, Mater. Sci. Forum 584−586 (2008) 748.
[7] J. Bohlen, S.B. Yi, J. Swiostek, D. Letzig, H.-G. Brokmeier, K.U. Kainer, Scrip. Mater. 53 (2005) 259.
[8] W.M. Gan, M.Y. Zheng, H. Chang, X.J. Wang, X.G. Qiao, K. Wu, B. Schwebke, H.-G. Brokmeier, J. Alloys Comp. 470 (2009) 256.
[9] Y. Harai, M. Kai, K. Kaneko, Z. Horita, T.G. Langdon, Mater. Trans. 49 (2008) 76.
[10] H.-G. Brokmeier, Mater. Sci. Forum 408−412 (2002) 149.
[11] H.-G. Brokmeier, W.M. Gan, C. Randau, M. Voeller, J. Rebelo-Kornmeier, M. Hofmann, Nucl. Instr. Meth. Phys. Res A642 (2011) 87.
[12] C. Randau, U. Garbe, H.-G. Brokmeier, J Appl. Cryst. 44 (2011) 641.
[13] Y.N. Wang, J.C. Huang, Mater. Chem. Phys. 81 (2003) 11.
[14] A. Yamashita, D. Yamaguchi, Z. Horita, T.G. Langdon, Mater. Sci. Eng. A287 (2000) 100.